Diabetologia (2010) 53:2417–2430
DOI 10.1007/s00125-010-1840-7

ARTICLE

Chronically increased glucose uptake by adipose tissue leads to lactate production and improved insulin sensitivity rather than obesity in the mouse

S. Muñoz · S. Franckhauser · I. Elias · T. Ferré · A. Hidalgo · A. M. Monteys · M. Molas · S. Cerdán · A. Pujol · J. Ruberte · F. Bosch

Received: 29 March 2010 / Accepted: 28 May 2010 / Published online: 10 July 2010

Abstract
Aims/hypothesis In adipocytes, triacylglycerol synthesis depends on the formation of glycerol 3-phosphate, which originates either from glucose, through glycolysis, or from lactate, through glyceroneogenesis. However, glucose is traditionally viewed as the main precursor of the glycerol backbone and thus, enhanced glucose uptake would be expected to result in increased triacylglycerol synthesis and contribute to obesity.
Methods To further explore this issue, we generated a mouse model with chronically increased glucose uptake in adipose tissue by expressing *Gck*, which encodes the glucokinase enzyme.
Results Here we show that the production of high levels of glucokinase led to increased adipose tissue glucose uptake and lactate production, improved glucose tolerance and higher whole-body and skeletal muscle insulin sensitivity. There was no parallel increase in glycerol 3-phosphate synthesis in vivo, fat accumulation or obesity. Moreover, at high glucose concentrations, in cultured fat cells overproducing glucokinase, glycerol 3-phosphate synthesis from pyruvate decreased, while glyceroneogenesis increased in fat cells overproducing hexokinase II.
Conclusions/interpretations These findings indicate that the absence of glucokinase inhibition by glucose 6-phosphate probably led to increased glycolysis and blocked

S. Muñoz and S. Franckhauser contributed equally to this study.

Electronic supplementary material The online version of this article (doi:10.1007/s00125-010-1840-7) contains supplementary material, which is available to authorised users.

S. Muñoz · S. Franckhauser · I. Elias · T. Ferré · A. Hidalgo · A. M. Monteys · M. Molas · A. Pujol · J. Ruberte · F. Bosch
Center of Animal Biotechnology and Gene Therapy, Edifici H,
Universitat Autònoma de Barcelona,
Bellaterra, Spain

S. Muñoz · I. Elias · A. Hidalgo · A. M. Monteys · A. Pujol · F. Bosch
Department of Biochemistry and Molecular Biology,
School of Veterinary Medicine,
Universitat Autònoma de Barcelona,
Bellaterra, Spain

S. Muñoz · S. Franckhauser · I. Elias · T. Ferré · M. Molas · A. Pujol · J. Ruberte · F. Bosch (✉)
CIBERDEM Spain
URL: www.ciberdem.net
e-mail: fatima.bosch@uab.es

S. Cerdán
Instituto de Investigaciones Biomédicas 'Alberto Sols' Consejo Superior de Investigaciones Científicas/
Universidad Autónoma de Madrid,
Madrid, Spain

J. Ruberte
Department of Anatomy and Animal Health,
School of Veterinary Medicine,
Universitat Autònoma de Barcelona,
Bellaterra, Spain

glyceroneogenesis in the mouse model. Furthermore, this study suggests that under physiological conditions, when blood glucose increases, glyceroneogenesis may prevail over glycolysis for triacylglycerol formation because of the inhibition of hexokinase II by glucose 6-phosphate. Together these results point to the indirect pathway (glucose to lactate to glycerol 3-phosphate) being key for fat deposition in adipose tissue.

Keywords Adipose tissue · Glucose metabolism · Glucose uptake · Glyceroneogenesis · Lipid metabolism · Transgenic mice

Abbreviations

BAT	Brown adipose tissue
EC_{50}	Half maximal effective concentration
GFP	Green fluorescent protein
GK	Glucokinase
HKII	Hexokinase II
NMR	Nuclear magnetic resonance
PPARγ2	Peroxisome proliferator-activated receptor γ2
PEPCK	Phosphoenolpyruvate carboxykinase
RBP-4	Retinol binding protein-4
WAT	White adipose tissue

Introduction

Obesity is a growing problem in Western society, and is associated with type 2 diabetes, insulin resistance, hypertension and dyslipidaemia. Obesity results from an imbalance between energy intake and expenditure, leading to increased energy storage in the form of triacylglycerol in white adipose tissue (WAT). Adipocytes synthesise triacylglycerol by esterification of non-esterified fatty acids with glycerol 3-phosphate; net lipid deposition occurs when the rate of esterification is higher than the rate of lipolysis. The synthesis of triacylglycerol depends on the formation of glycerol 3-phosphate, which may originate either from glucose through glycolysis, or from lactate and pyruvate through glyceroneogenesis [1–3]. Overproduction of the key enzyme of glyceroneogenesis, phosphoenolpyruvate carboxykinase (PEPCK), in adipose tissue leads to increased glycerol 3-phosphate, NEFA re-esterification, adipocyte hypertrophy and obesity [4]. This is associated with higher susceptibility to diet-induced insulin resistance and obesity [5]. In contrast, the ablation of PEPCK in adipose tissue leads to reduced triacylglycerol deposition and lipodystrophy [6]. In addition, although there are few studies of the relative contribution of pyruvate, via glyceroneogenesis, vs glucose, via glycolysis, to glyceride–glycerol synthesis, it has been demonstrated that glyceroneogenesis is quantitatively the predominant source of glycerol in triacylglycerol [7, 8]. However, glucose is still traditionally viewed as the main precursor of the glycerol backbone.

Glucose transport is considered a key regulatory step in insulin-stimulated glucose utilisation in adipocytes. In obesity and type 2 diabetes, insulin resistance leads to decreased adipose tissue glucose uptake, which parallels the downregulation of glucose transporter 4 production in adipose tissue [9–12]. In adipose-specific *Glut4* (also known as *Slc2a4*) knockout mice, insulin-stimulated glucose transport, glucose disposal and insulin sensitivity in adipose tissue are impaired [13–15]. Thus, a primary defect in adipocyte glucose uptake induces insulin resistance in other insulin-target tissues, probably through a factor secreted by adipose tissue, such as retinol binding protein-4 (RBP-4) [13, 14, 16]. Nevertheless, despite a marked decrease in glucose transport, these mice do not show differences in adipose mass and adipocyte size [13, 14]. This suggests that lipid synthesis in adipose tissue is not dependent on insulin-stimulated glucose uptake. However, increased insulin-stimulated glucose uptake in adipose tissue from transgenic mice overexpressing *Glut4* in adipocytes leads to higher fat mass, though the main part of the glucose is metabolised to lactate (70%) [17–19]. In addition to glucose transport, glucose utilisation also depends on glucose phosphorylation. In adipocytes, glucose is mainly phosphorylated by hexokinase II (HKII) which, together with GLUT4, controls insulin-stimulated glucose utilisation. Hexokinase II is considered regulatory when glucose transport is maximally stimulated, through feedback inhibition of the enzyme by glucose 6-phosphate [20–22].

Therefore, we hypothesised that enhanced glucose uptake and metabolism in adipose tissue would result in increased triacylglycerol synthesis and contribute to obesity. Thus, transgenic mice were engineered to increase adipose tissue glucose phosphorylation by producing the liver enzyme glucokinase (GK). In contrast to HKII, GK has a high K_m for glucose (5–8 mmol/l) and its activity is not inhibited by glucose 6-phosphate [23]. We found that in transgenic mice expressing *Gck*, increased glucose uptake in adipose tissue did not lead to higher glycerol 3-phosphate levels and fat mass, but to an increase in lactate production and to improved whole-body insulin sensitivity and glucose tolerance.

Methods

Generation of transgenic mice A 3.1 kb XmaI-NotI fragment containing the rat hepatic *Gck* cDNA and the polyadenylation signal of the SV40 virus was introduced downstream of the *Ap2* (also known as *Fabp4*) promoter at the XmaI-NotI site in the p*Ap2* plasmid [24, 25]. The entire

Ap2–Gck chimeric gene (8.5 kb) was microinjected into fertilised eggs as described by our group elsewhere [4]. Mice were tested for the presence of the transgene by Southern blot with a probe radiolabelled with deoxycytidine 5′-[^{32}P]triphosphate (Amersham Pharmacia Biotech, Piscataway, NJ, USA) by random oligopriming (Amersham). C57Bl6/SJL mice were fed ad libitum with a standard diet (Panlab, Barcelona, Spain) and maintained under a light–dark cycle of 12 h (lights on at 09:00). When stated, mice were starved for 16–18 h. Isofluorane-anaesthetised mice were killed by decapitation and samples were taken between 09:00 and 10:00. In the experiments described below, male mice, aged 4 and 6 months, were used. We used littermates as controls. Control and transgenic male mice aged 2 months were kept in individual cages and fed a high-fat diet (TD 88137; Tekland, Madison, WT, USA) or a standard diet for up to 11 weeks. All experimental procedures involving mice were approved by the Ethics and Experimental Animal Committee of the Universitat Autònoma de Barcelona, Spain.

Cell culture and transient transfection of 3T3-L1 adipocytes and adipocytes isolation 3T3-L1 pre-adipocytes were cultured and differentiated as previously described with some modification [26] and as detailed in the Electronic supplementary material (ESM). Transient transfection of 3T3-L1 cells was performed using Lipofectamine 2000 (Invitrogen Life Sciences, Carlsbad, CA, USA) according to the manufacturer's instructions with some modifications as detailed in the ESM. Briefly, differentiated cells were incubated for 24 h with a mixture of DNA/lipofectamine (respectively 7 μg and 7 μl per well of six well plates) in Opti-MEM medium (Invitrogen). Isolation of adipocytes from epididymal fat pad was performed using a modification of the Rodbell's method [27] as detailed in the ESM.

RNA and protein analysis Total RNA was obtained as previously described by our group [4]. Northern blot, RT-PCR using Omniscript Reverse transcriptase kit (Qiagen, Hilden, Germany) and real-time quantitative PCR using QuantiTect SYBR Green (Qiagen) and SmartCyclerII II (Cepheid, Sunnyvale, CA, USA) was performed following the manufacturers' instructions and as detailed in the ESM. The sequences of oligonucleotide primers are given in the ESM (ESM Table 1). Western blot analysis was performed using standard procedures with total homogenates of WAT, skeletal muscle and liver [4]. The antibodies used are described in the ESM.

Metabolic studies using radiolabelled tracers The in vivo glucose utilisation index in epididymal WAT was determined by the intravenous flash injection of deoxy-D-[^{3}H]glucose (Amersham) as previously described by Franckhauser et al. [4]. Uptake of deoxy-D-[^{3}H]glucose was measured in isolated soleus muscles, in 3T3-L1 adipocytes and in isolated-adipocyte suspension incubated with or without insulin as previously described [4, 28, 29] and in the ESM. To determine glucose and pyruvate incorporation into lipids, epididymal fat pads and 3T3-L1 adipocytes were incubated for 2 h with either D-[U-^{14}C]glucose or D-[2-^{14}C]pyruvate (PerkinElmer, Waltham, MA, USA) supplemented with glucose as stated in the figure legends. Total lipids, fatty acids and glyceride–glycerol were then isolated as previously described [4]. For in vivo pyruvate incorporation, mice were given an intraperitoneal injection of [2-^{14}C]pyruvate and glyceride–glycerol was extracted. Incorporation of ^{14}C radioactivity was measured and corrected by specific blood pyruvate ^{14}C clearance.

Body fat content and histological analysis The fat content of mouse carcasses was measured as previously described by Salmon and Flatt [30]. Epididymal fat pads were fixed for 12–24 h in formalin, embedded in paraffin and then sectioned. Sections were stained with haematoxylin/eosin. Quantification of adipocyte size in white adipose tissue and laser-scanning confocal microscopy studies in isolated adipocytes were performed as described in the ESM.

Lactate synthesis from glucose in transgenic mice To investigate in vitro lactate production, epididymal fat pads were incubated in Krebs–Ringer bicarbonate HEPES buffer with 20 mmol/l glucose, and lactate concentrations were measured in the incubation medium at the times indicated. To measure in vivo lactate release, starved mice were given an intraperitoneal injection of glucose and blood samples were obtained from the tail vein before and after the injection. Glucose and lactate concentration were measured in blood samples and incubation media as described in the ESM. For the ^{13}C- nuclear magnetic resonance (NMR) experiment, mice received an intraperitoneal injection of [1-^{13}C]glucose and NMR was performed in perchloric acid extracts of WAT as detailed in the ESM.

Intraperitoneal glucose and insulin tolerance tests Glucose and insulin tolerance tests were performed as previously described [4] and in the ESM. Conscious mice were given an intraperitoneal injection of either glucose or insulin and blood glucose levels were measured from samples obtained by tail vein bleeding before the injection and afterwards at the time points indicated.

Metabolite and hormones assays For metabolite assays in epididymal WAT, gastrocnemius and liver, tissues biopsies were obtained from anaesthetised mice and frozen. Hormone and metabolite concentrations were determined as indicated in the ESM.

Statistical analysis All values are expressed as the means ± SEMs. The significance of differences between data was analysed using the Student–Newman–Keuls test. Differences were considered significant at $p<0.05$.

Results

Adipose-specific expression of glucokinase led to increased glucose uptake Two independent transgenic lines (Tg1 and

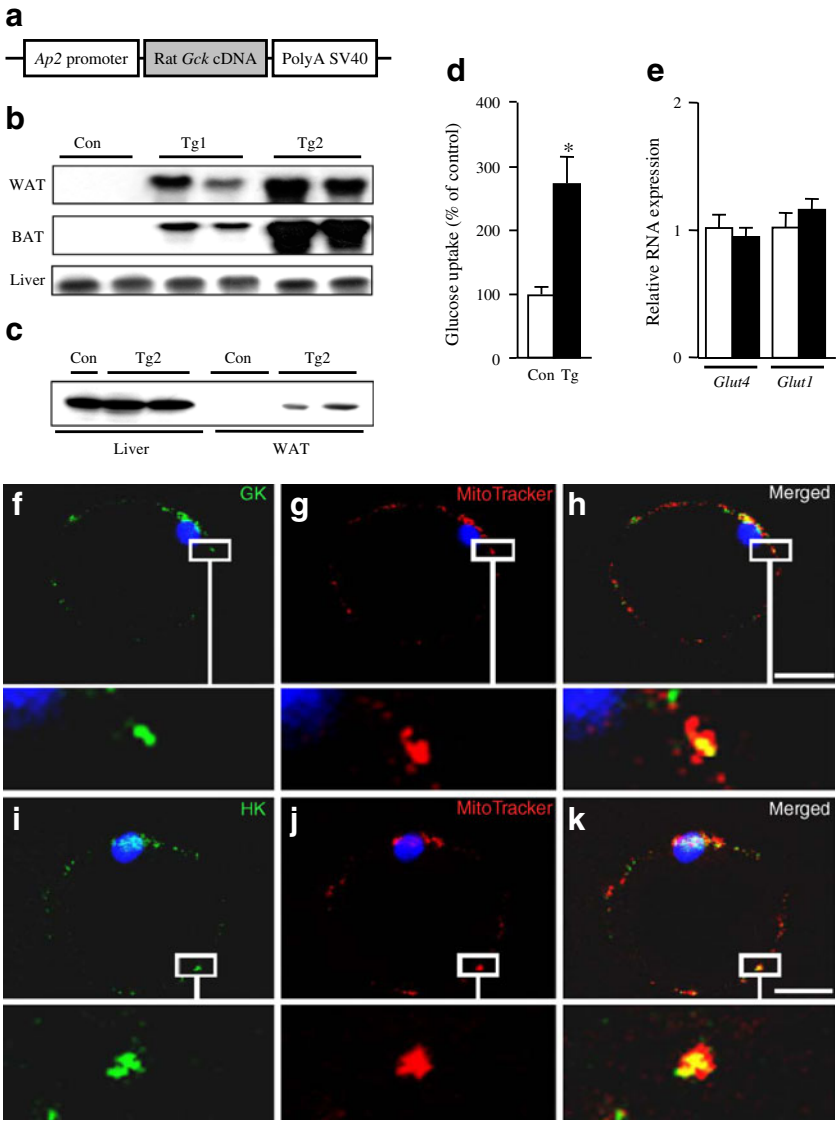

Fig. 1 Adipose-specific production of glucokinase and in vivo basal glucose uptake in adipose tissue of *Gck*-expressing transgenic mice (Tg) and control mice (Con). **a** Schematic representation of the *Ap2–Gck* chimeric gene. **b** Expression of the transgene in WAT and BAT. Representative northern blots from epididymal WAT, interscapular BAT and liver from control and heterozygous transgenic mice from line 1 (Tg1) and line 2 (Tg2), hybridised with a *Gck* probe are shown. **c** Protein levels of GK were detected by Western blots of epididymal WAT and liver from control and heterozygous transgenic mice from line 2 (Tg2). A representative western blot is shown. **d** The glucose utilisation index was measured in epididymal white adipose tissue of fed control and transgenic mice, as indicated in the text and the ESM. Results are presented as percentage of basal glucose utilisation in WAT of control mouse (302.13 pmol[mg protein]$^{-1}$ min^{-1}). The results are the means ± SEMs from at least four mice for each group. *$p<0.05$. **e** Expression of glucose transporter genes *Glut1* (also known as *Slc2a1*) and *Glut4* in epididymal WAT. The quantification of the level of expression was performed by real-time quantitative PCR using SYBR Green as indicated in the text and the ESM. Data were normalised with *36B4* (also known as *Rplp0*) values and analysed as described in the text and the ESM. Results are means ± SEM of data from three mice for each group. Control mice, white bars; transgenic mice, black bars. **f–k** Representative laser-scanning confocal images in isolated transgenic adipocytes. Co-localisation (**h**, **k**) of GK (**f**) and HKII (**i**) with mitochondria (**g**, **j**). GK and HKII were marked with green fluorescent Alexa 488 and mitochondria with orange rosamine MitoTracker. Nuclei of adipocytes were marked with blue Hoechst stain solution. Note that hexokinases and mitochondria surround an empty space corresponding to the unilocular lipid droplet. Scale bar, 11 μm

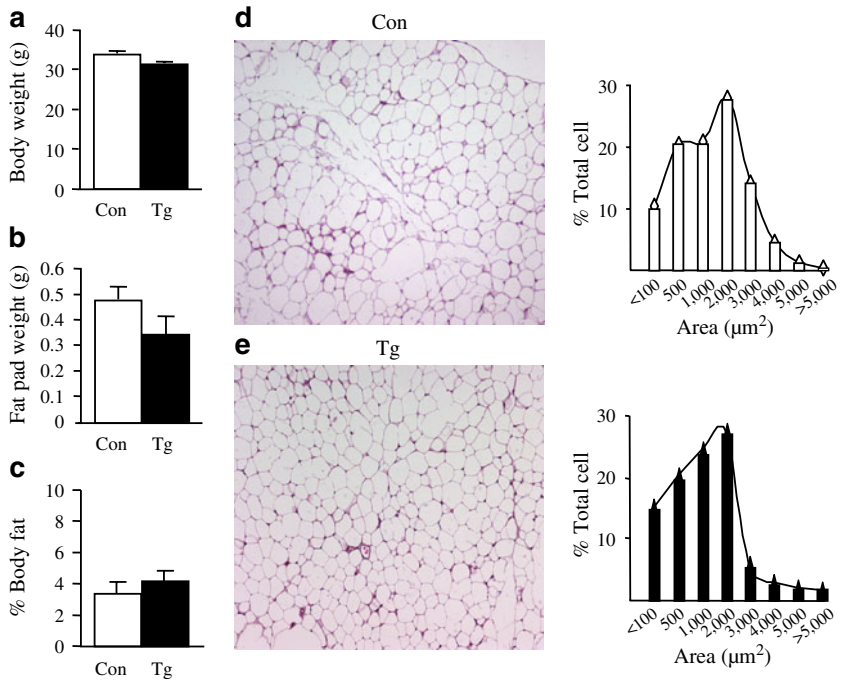

Fig. 2 Adiposity analysis in transgenic mice expressing *Gck* (Tg) and control mice (Con). Body weight (**a**) and epididymal fat pad weight (**b**) from 4-month-old male control mice and heterozygous transgenic mice. **c** Body fat content expressed as % body weight was measured as described in the text and the ESM. Results are means ± SEMs from six to eight mice for each group. **d, e** Representative sections stained with haematoxylin/eosin of epididymal WAT from control mice (**d**) and transgenic mice (**e**) (magnification ×10). Frequency distribution of adipocyte cell surface area from epididymal white adipose tissue of control mice (**f**) (mean=1,024±812 μm^2) and heterozygous transgenic mice (**g**) (mean=940±743 μm^2). Results are means ± SEMs from 3,748 adipocytes from control mice and 5,015 adipocytes from transgenic mice

Tg2) expressing hepatic *Gck* under control of the adipose-specific *aP2* promoter were obtained (Fig. 1a). Transgenic mice showed high levels of *Gck* mRNA in white adipose tissue and brown adipose tissue (BAT; Fig. 1b). Furthermore, GK protein was detected in the WAT of Tg2 mice, whereas no GK was noted in the controls (Fig. 1c). In addition, the level of GK protein in the WAT of Tg2 mice was 20% that of the endogenous hepatic GK level. While skeletal muscle from both control and transgenic mice did not produce GK (results not shown), liver from both groups showed a 2.3 kb mRNA transcript (Fig. 1b) resulting from the expression of the endogenous hepatic *Gck* gene. Moreover, similar levels of GK protein were detected in the livers of both control and transgenic mice, indicating the adipose specificity of the transgene (Fig. 1c). The transgenic line with highest *Gck* expression, Tg2, was used in this study.

In WAT, a significant increase (about 2.5-fold) in the glucose utilisation index, evaluated by measuring 2-deoxy-

Table 1 Serum and liver variables in fed and starved control and transgenic mice

Biochemical variable	Fed		Starved	
	Control	Transgenic	Control	Transgenic
Insulin (pmol/l)	126.75±6.95	128.48±24.31	34.73±5.21	39.93±6.95
Adiponectin (μg/ml)	5.24±0.43	5.81±0.65	5.79±0.53	5.47±0.60
Leptin (pmol/l)	287.5±73.1	331.3±110.0	15.0±6.3	8.8±3.8
Serum triacylglycerol (mmol/l)	1.55±0.29	1.29±0.35	1.09±0.09	1.07±0.11
Serum NEFA (mmol/l)	0.9±0.15	1.1±0.08	1.9±0.15	1.8±0.14
Serum glycerol (μmol/l)	293±35	262±21	ND	ND
Serum β-hydroxybutyrate (mmol/l)	1.04±0.17	0.79±0.11	ND	ND
Liver glucose 6-phosphate (μmol/g)	1.30±0.20	1.13±0.14	0.30±0.08	0.20±0.04
Liver glycogen (μmol glucose/g)	136.7±25.3	112.6±12	1.2±0.7	4.5±0.7*
Liver triacylglycerol (μmol/g)	5.14±0.80	7.20±0.46*	27.54±4.69	21.72±2.86

Results are means ± SEMs from at least eight mice for each group

* $p<0.05$ vs matched control

ND, not determined

[1-^{3}H]glucose uptake in vivo, was observed in transgenic mice (Fig. 1d). In addition, production of glucose transporters 1 and 4 in the adipose tissue of transgenic mice was similar to that in controls (Fig. 1e). This suggests that the specific increase in adipose tissue glucose uptake in transgenic mice was due to the presence of GK in WAT.

In order to examine the subcellular localisation of GK, the percentage of co-localisation of GK with mitochondria was determined and compared with that of endogenous hexokinase, HKII. To this end, both enzymes were immunodetected in isolated adipocytes from transgenic mice and visualised by laser-scanning confocal microscopy (Fig. 1f–k). In transgenic mice, similar percentages of HKII and GK co-localised with mitochondria (HKII, 41.05±9.58% vs GK, 39.37±15.88%; n=12), indicating a similar subcellular distribution.

Glucokinase production in adipose tissue does not increase adiposity The effect of glucokinase production on lipid storage in adipose tissue was further examined. Body weight, epididymal fat pad weight and body fat content were similar in transgenic and control mice (Fig. 2a–c). Moreover, the frequency of distribution and mean adipocyte size from control and transgenic mice were similar (Fig. 2d–g). These findings indicate that the transgenic mice did not develop adipose tissue hypertrophy and/or hyperplasia.

Similarly, in agreement with the lack of extra fat accumulation in transgenic mice, serum levels of adiponectin and leptin, as well as circulating NEFA, glycerol, triacylglycerol and β-hydroxybutyrate in the transgenic mice were similar to those in the controls (Table 1).

Increased glucose uptake in adipose tissue does not lead to increased glycerol 3-phosphate synthesis In ex vivo epididymal WAT from transgenic mice, [^{14}C]glucose conversion into lipids, fatty acids or glyceride–glycerol synthesis

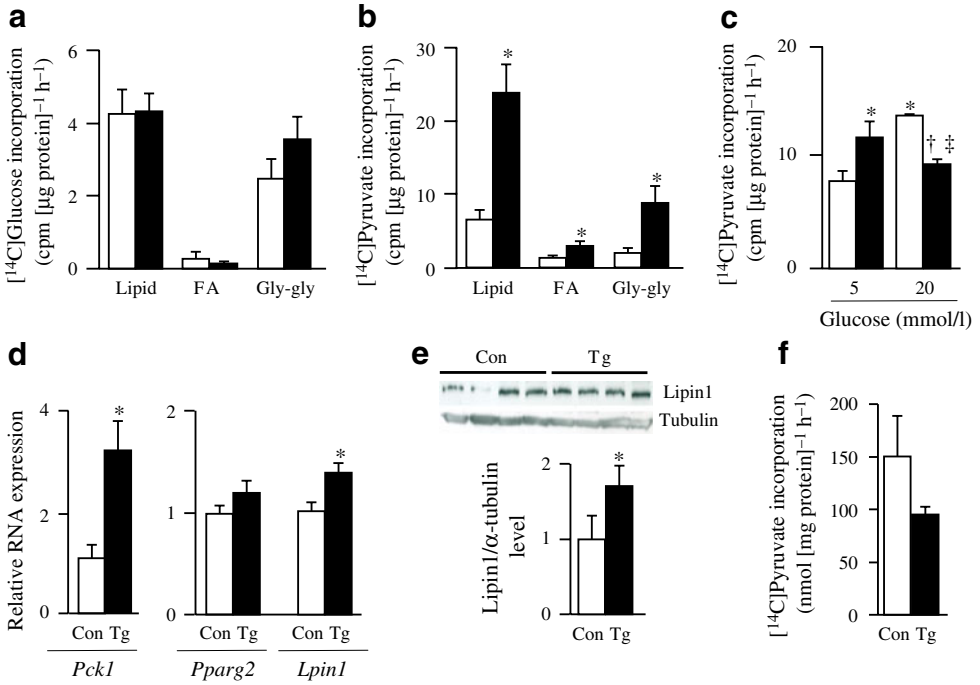

Fig. 3 Glycerogenesis and glyceroneogenesis in *Gck*-expressing transgenic mice (Tg, black bars) and control mice (Con, white bars). **a** In vitro D-[U-^{14}C]glucose conversion into lipids, fatty acid and glyceride–glycerol (glycerogenesis) in epididymal WAT explants from 4-month-old control and transgenic mice. Incubation media were supplemented with 5 mmol/l non-labelled glucose. **b** In vitro D-[2-^{14}C] pyruvate conversion into lipids, fatty acid and glyceride–glycerol (glyceroneogenesis) in epididymal WAT explants from control and transgenic mice. Incubation media were not supplemented with non-labelled glucose. **c** In vitro D-[2-^{14}C]pyruvate conversion into glyceride–glycerol (glyceroneogenesis) in epididymal WAT explants from control and transgenic mice in the presence of non-labelled glucose. Incubation media were supplemented with 5 mmol/l or 20 mmol/l non-labelled glucose. *p<0.05 vs control, 5 mmol/l glucose; †p<0.05 vs control, 20 mmol/l glucose; and ‡p<0.05 vs transgenic, 5 mmol/l glucose. **d** *Pck1*, *Pparg2* and *Lpin*1 expression in epididymal WAT from control and transgenic mice was quantified by real-time quantitative PCR as described in the text and the ESM. **e** Representative western blot of lipin1 protein levels in epididymal WAT from fed control and transgenic mice. Densitometric quantification of Lipin1 protein levels was performed using α-tubulin protein levels as a loading control. **f** In vivo D-[2-^{14}C]pyruvate conversion into glyceride–glycerol in epididymal WAT from control and transgenic mice. Results of in vivo and WAT explant studies are means ± SEMs from at least five 4-month-old mice for each group. Real-time quantitative PCR data were normalised with 36B4 values and results are means ± SEMs from at least four mice for each group. Densitometry of western blot results are means ± SEMs from eight 4-month-old mice for each group. FA, fatty acid; Gly-gly, glyceride–glycerol. *p<0.05 vs control unless otherwise specified

(glycerogenesis) in the presence of 5 mmol/l non-labelled glucose was not altered compared with control mice (Fig. 3a). Similar results were observed in the presence of 20 mmol/l glucose (data not shown).

The alternative pathway involved in glyceride–glycerol synthesis, glyceroneogenesis, was also examined. In the absence of glucose, WAT explants from transgenic mice had higher rates of pyruvate incorporation into lipid, fatty acids or glyceride–glycerol (Fig. 3b). In the presence of 5 mmol/l glucose, [^{14}C]pyruvate incorporation into glyceride–glycerol was increased in WAT explants producing GK compared with control WAT (Fig. 3c). At high concentrations of glucose (20 mmol/l), the pyruvate conversion rate was further increased in WAT from control mice while it decreased in WAT from transgenic mice (Fig. 3c). Moreover, the increase in glyceroneogenesis observed in transgenic mice was parallel to higher expression of *Pepck* (Fig. 3d). However, expression of the main *Pepck* adipo-specific transcriptional regulator, peroxisome proliferator-activated receptor γ2 (PPARγ2) remained unchanged (Fig. 3d). In contrast, a significant increase in the expression of both *Lipin1* (also known as *Lpin1*) mRNA and protein, a factor specifically recruited to the PPARγ$_2$-response element of the *Pepck* promoter, was observed in WAT from transgenic mice (Fig. 3d, e) [31]. However, despite an increase in both *Pepck* expression and in the glyceroneogenic rate observed in vitro, no change was observed in fat accumulation in these mice. Thus, labelled pyruvate incorporation into glyceride–glycerol was measured in vivo in fed control and transgenic mice. Under these conditions, the glyceroneogenic rate was similar in control and transgenic mice (Fig. 3f).

In order to evaluate the effect of glucose on pyruvate incorporation into lipids and glyceride–glycerol, as well as

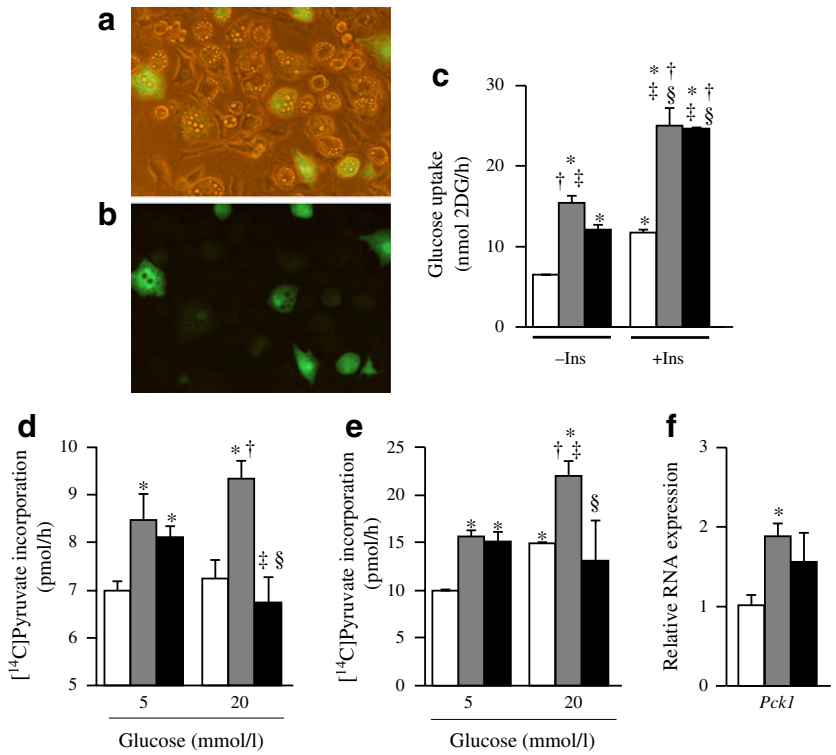

Fig. 4 In vitro glucose uptake and glyceroneogenesis in differentiated and transiently transfected 3T3-L1 adipocytes. **a**, **b** Differentiated and transiently transfected 3T3-L1 adipocytes with pCMV-GFP were observed by bright-field (**a**) and fluorescent (**b**) microscopy. Representative images are shown. **c** In vitro 2-deoxy-D-[1-^{3}H]glucose (2DG) uptake in differentiated and transiently transfected 3T3-L1 adipocytes with pCMV-SV40 (null, white bar), pCMV-mHKII (HK, grey bar) or pCMV-rGK (GK, black bar) without insulin (−Ins) or with 20 nmol/l insulin (+Ins). *p<0.05 vs null −Ins; $^{\dagger}p$<0.05 vs null +Ins; $^{\ddagger}p$<0.05 vs GK −Ins; and $^{\S}p$<0.05 vs HK −Ins. **d** D-[2-^{14}C]pyruvate conversion into glyceride–glycerol in differentiated and transiently transfected 3T3-L1 adipocytes with pCMV-SV40 (null, white bar), pCMV-mHKII (HK, grey bar) or pCMV-rGK (GK, black bar) with 5 and 20 mmol/l non-labelled glucose. *p<0.05 vs null, 5 mmol/l glucose; $^{\dagger}p$<0.05 vs null, 20 mmol/l glucose; $^{\ddagger}p$<0.05 vs GK, 5 mmol/l glucose; and $^{\S}p$<0.05 vs HK, 20 mmol/l glucose. **e** D-[2-^{14}C]pyruvate conversion into lipids in differentiated and transiently transfected 3T3-L1 adipocytes with pCMV-SV40 (null, white bar), pCMV-mHKII (HK, grey bar) or pCMV-rGK (GK, black bar) with 5 mmol/l and 20 mmol/l non-labelled glucose. *p<0.05 vs null, 5 mmol/l glucose; $^{\dagger}p$<0.05 vs null, 20 mmol/l glucose; $^{\ddagger}p$<0.05 vs HK, 5 mmol/l glucose; and $^{\S}p$<0.05 vs HK, 20 mmol/l glucose. **f** *Pck1* gene expression in differentiated and transiently transfected 3T3-L1 adipocytes with pCMV-SV40 (null, white bar), pCMV-mHKII (HK, grey bar) or pCMV-rGK (GK, black bar) was quantified by real-time quantitative PCR as indicated in the text and the ESM. 3T3-L1 adipocyte results are means ± SEMs of three dishes for each group. *p<0.05 vs null

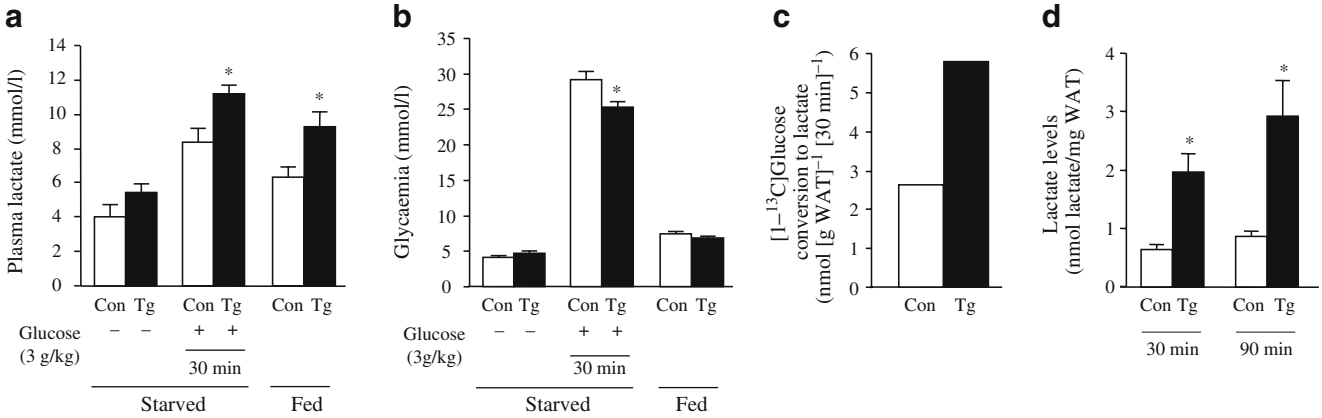

Fig. 5 Lactate and glucose levels in *Gck*-expressing transgenic (Tg) mice and control (Con) mice. In vivo plasma lactate levels (**a**) and blood glucose (**b**) of fed and overnight-fasted control and transgenic mice before and 30 min after an intraperitoneal injection of 3 g glucose per kg body weight. Results are means ± SEMs from at least six mice for each group. **c** Intracellular lactate was measured from ^{13}C-NMR spectra of WAT extracts using a standard solution ([^{13}C] lactate, 0.22 mmol/l). Results were obtained from pools of five mice for each group as indicated in the text and the ESM. **d** Ex vivo lactate release from adipose tissue. Epididymal WAT samples from fed control and transgenic mice were isolated and incubated with 20 mmol/l glucose. Lactate levels in the medium were measured after 30 and 90 min of glucose incubation, as indicated in the text and the ESM. Results are means ± SEMs from at least four mice for each group. *p<0.05 vs control

to study the effect of overproduction of the key endogenous enzyme in glucose phosphorylation, HKII, 3T3-L1 adipocytes were transiently transfected to produce GK, HKII or green fluorescent protein (GFP) as a control of transfection (Fig. 4a, b). In cells overexpressing either *HkII* (also known as *Hk2*) or *Gck*, 2-deoxyglucose uptake was increased (Fig. 4c). In the presence of 5 mmol/l glucose, [^{14}C]pyruvate incorporation into glyceride–glycerol and lipids, and *Pepck* expression were increased in cells overexpressing *Gck* or *HkII* compared with control cells (Fig. 4d–f). At the high concentration of glucose (20 mmol/l), the pyruvate conversion rate increased in *HkII*-expressing cells while the glyceroneogenic rate was decreased in *Gck*-expressing adipocytes (Fig. 4d, e). This suggests that, at high glucose concentration, the inhibition of HKII activity by glucose 6-phosphate leads to an increase in glyceroneogenesis, whereas an increase in glycolytic flux due to GK activation leads to a decrease in glyceroneogenesis.

Increased glucose uptake in adipose tissue leads to higher lactate formation The effect of an increase in adipose glucose uptake on circulating lactate levels was further examined. Plasma lactate levels were increased in fed but not starved transgenic mice (Fig. 5a), whereas glucose levels were not altered (Fig. 5b). Lactate concentrations increased in starved transgenic and control mice at 30 min after a glucose injection (Fig. 5a). However, lactate levels were higher in transgenic mice than in control mice, though blood glucose levels were lower (Fig. 5b). This is as would be expected if glucose uptake by adipose tissue had increased. The fate of glucose in adipose tissue was then confirmed by ^{13}C-NMR spectroscopy. The main difference

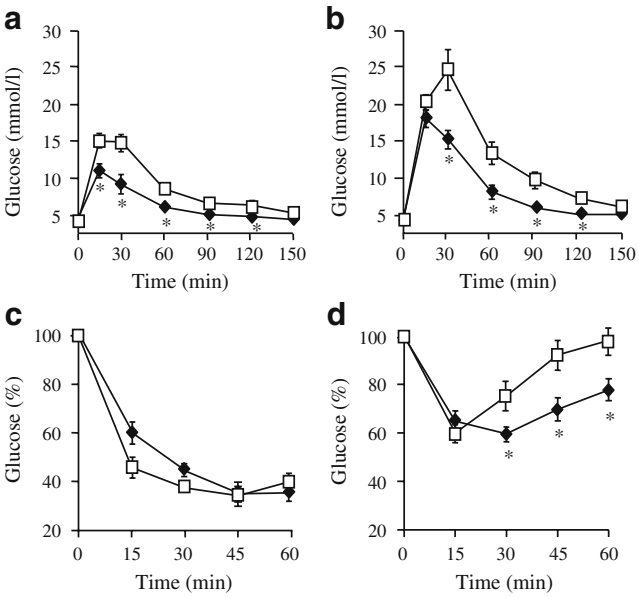

Fig. 6 Glucose homeostasis and whole-body insulin sensitivity in *Gck*-expressing transgenic mice (Tg) and control mice (Con). **a**, **b** Glucose tolerance test. Awake overnight-fasted control mice and transgenic mice were given an intraperitoneal injection of glucose at 1 g/kg body weight (**a**) and 2 g/kg body weight (**b**). Blood samples were taken at the times indicated from the tail vein of the same animal. **c**, **d** Insulin tolerance test. Insulin at 0.75 U per kg body weight (**c**) or 0.375 U per kg body weight (**d**) was injected intraperitoneally into awake fed mice. Blood samples were taken from the tail vein of the same animals at the times indicated and glucose levels were determined. Results of tolerance tests are means ± SEMs from at least eight mice for each group. Control mice, white squares; transgenic mice, black diamonds. *p<0.05 vs control

between the ^{13}C spectra of WAT from transgenic and control mice were higher levels of [3-^{13}C]lactate in transgenic extracts, indicating an increase (about twofold) in [1-^{13}C]glucose conversion to lactate (Fig. 5c). When adipose tissue explants were incubated in the presence of glucose, higher levels of lactate accumulated in the incubation medium of WAT from transgenic mice than in the medium with WAT from control mice (Fig. 5d). This occurred in parallel with a decrease in glucose concentration in the medium (data not shown).

Metabolic changes in the liver of Gck-expressing mice The effect of the increased circulating lactate concentration on hepatic metabolism was examined next. No change in hepatic glucose 6-phosphate content was observed in control and transgenic mice kept under either fed or starved conditions (Table 1). However, during starvation, transgenic mice had higher levels of hepatic glycogen (about fourfold) than those of controls. In addition, under fed conditions, transgenic livers had a higher triacylglycerol content (by about 40%) than controls (Table 1). These results suggest that lactate released by adipose tissue may have contributed to glycogen and triacylglycerol synthesis in the liver.

Glucose homeostasis in glucokinase-expressing transgenic mice It has been suggested that high levels of circulating lactate observed during obesity may contribute to insulin resistance [32–37]. However, no difference in serum insulin concentration was observed in fed or starved transgenic mice compared with controls (Table 1). An intraperitoneal glucose tolerance test was also performed. After injecting glucose at 1 or 2 g per kg body weight, glycaemia reached a lower level in transgenic mice compared with controls, indicating higher glucose disposal in the transgenic mice (Fig. 6a, b). In addition, insulin sensitivity was measured by insulin tolerance tests at two doses of insulin (0.75 and 0.375 U/kg body weight). Fed control and transgenic mice showed similar responses to a high dose of insulin (Fig. 6c). However, when the lower dose of insulin was injected, a hypoglycaemic response of greater magnitude was observed in transgenic mice (Fig. 6d). In order to determine whether glucokinase production led to increased insulin sensitivity

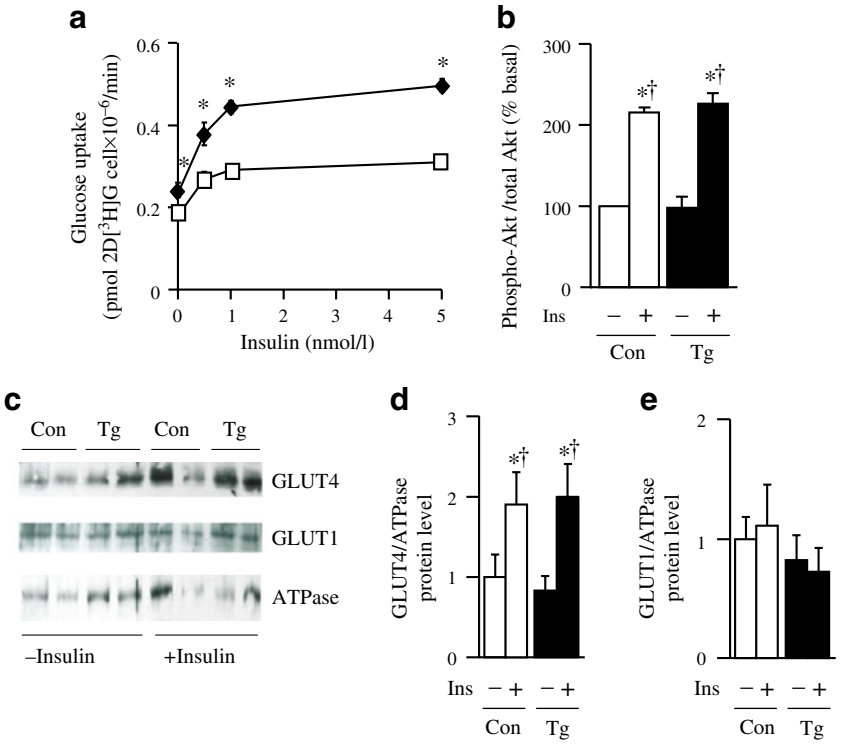

Fig. 7 Insulin sensitivity of adipose tissue in *Gck*-expressing transgenic mice (Tg) and control mice (Con). **a** The insulin dose/glucose-uptake response in isolated adipocytes from control mice (white squares) and transgenic mice (black diamonds) was analysed. $^{*}p<0.05$. **b** Densitometric quantification of phospho-AKT(Ser473) was normalised to total AKT protein levels by western blots of epididymal WAT from starved control mice and transgenic mice with (+) or without (−) insulin stimulation. **c** Representative western blots of GLUT4 and GLUT1 protein in the plasma membrane of epididymal WAT from starved control mice (Con) and transgenic (Tg) mice with (+) or without (−) insulin stimulation. **d, e** Densitometric quantification of GLUT4 (**d**) and GLUT1 (**e**) protein levels was performed using sodium potassium ATPase protein as the membrane loading control. The results are the means ± SEMs from at least four mice for each group. $^{*}p<0.05$ vs control −insulin; $^{\dagger}p<0.05$ vs transgenic −insulin. 2DG, 2-deoxy-D-[1-^{3}H]glucose

of adipose tissue, the response in glucose uptake to insulin dose in isolated adipocytes from control and transgenic mice was measured. Adipocytes from transgenic mice had higher rates of glucose uptake in the absence or presence of increasing doses of insulin (Fig. 7a). However, the half maximal effective concentration, EC_{50}, was similar in control and transgenic mice (control EC_{50} 0.32 nmol/l and transgenic EC_{50} 0.37 nmol/l). Similarly, in adipose tissue, basal and insulin-stimulated phosphorylation of protein kinase B/AKT on serine 473 remained unchanged (Fig. 7b). In addition, translocation of either of the GLUT4 or GLUT1 glucose transporters to the plasma membrane in response to insulin was not altered in transgenic mice compared with control mice (Fig. 7c–e).

In agreement with increased whole-body insulin sensitivity, insulin-stimulated glucose uptake was higher in skeletal muscle from transgenic mice (Fig. 8a). In addition, a slight increase in basal and insulin-stimulated phosphorylation of AKT was also observed in skeletal muscle from transgenic mice (Fig. 8b). The decreased expression of *Rbp4* in adipose tissue and the subsequent decrease in RBP-4 serum levels in transgenic mice may have contributed to higher insulin sensitivity in these mice (Fig. 8c, d).

Finally, in order to examine whether expression of *Gck* in adipose tissue prevents diet-induced insulin resistance, mice were fed a high-fat diet. Body weight gain, fat pad weight and histological analysis of WAT revealed similar fat accumulation between transgenic and control mice (Fig. 9a–d). In addition, serum levels of triacylglycerol, leptin and adiponectin remained unchanged between both groups (Fig. 9e–g). In contrast, circulating insulin levels tended to be lower in transgenic than in control mice, although mice remained normoglycaemic (Fig. 9h, i). Whole-body insulin sensitivity was also measured. In fat-fed control mice, the hypoglycaemic effect of insulin was reduced compared with control mice fed a chow diet, while the insulin response of fat-fed transgenic mice was similar to the control response (Fig. 9j). This indicates that transgenic mice, when fed a high-fat diet, became obese similarly to controls, but remained insulin sensitive.

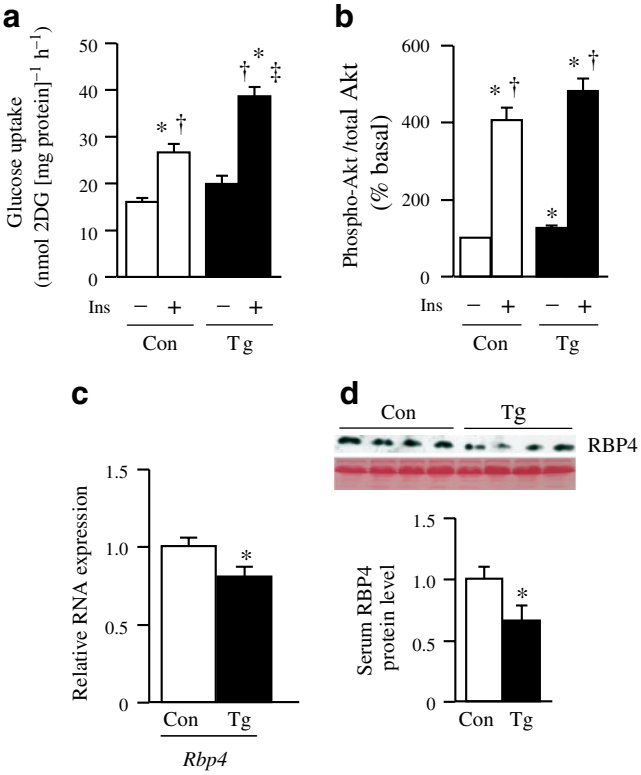

Fig. 8 Skeletal muscle insulin sensitivity and circulating serum RBP-4 levels in *Gck*-expressing transgenic mice (Tg) and control mice (Con). **a** Ex vivo insulin-stimulated glucose uptake in soleus skeletal muscle from starved control and transgenic mice. 2DG, 2-deoxy-D-[1-^{3}H]glucose **b** Densitometric quantification of phospho-AKT (Ser473) was normalised to total AKT protein levels by western blots of gastrocnemius skeletal muscle from control and transgenic mice with (+) or without (−) insulin stimulation. *p<0.05 vs control −insulin; †p<0.05 vs transgenic −Ins; and ‡p<0.05 vs control +Ins. **c** *Rbp4* gene expression in epididymal WAT from 4-month-old fed control and transgenic mice was quantified by real-time quantitative PCR as indicated in the text and the ESM. **d** Circulating serum RBP-4 protein levels from 4-month-old fed control and transgenic mice. Representative western blot of circulating RBP-4 protein levels from 2 μl serum samples. Densitometric quantification of circulating RBP-4 protein levels was performed by using Ponceau staining. The results from the ex vivo study, *Rbp4* expression and western blots of serum samples are means ± SEMs from at least four mice for each group. *p<0.05 vs control unless otherwise specified

Discussion

It is generally accepted that lipid storage in adipose tissue depends mainly on insulin-stimulated glucose uptake to generate the glycerol 3-phosphate necessary for fatty acid esterification. In this study we show that expression of *Gck* selectively in adipose tissue of transgenic mice leads to increased glucose uptake in this tissue, but not to glycerol 3-phosphate formation and fat accumulation. Furthermore, we demonstrated that the increased glucose flux in adipose tissue led to increased lactate release and higher circulating lactate levels within the physiological range. Similarly, in *Glut4*-overexpressing mice, the majority of glucose was metabolised to lactate (70%) [17]. This is also consistent with results obtained in transgenic mice expressing *Gck* in skeletal muscle or in the liver, in which serum lactate concentrations were increased [24, 29]. Moreover, in these mice, the increase of lactate production by hepatocytes occurred only at high glucose concentration [24]. Similarly, transgenic mice expressing *Gck* in adipose tissue displayed increased lactate levels only in fed conditions or after a glucose load. This probably reflects the potent activation of

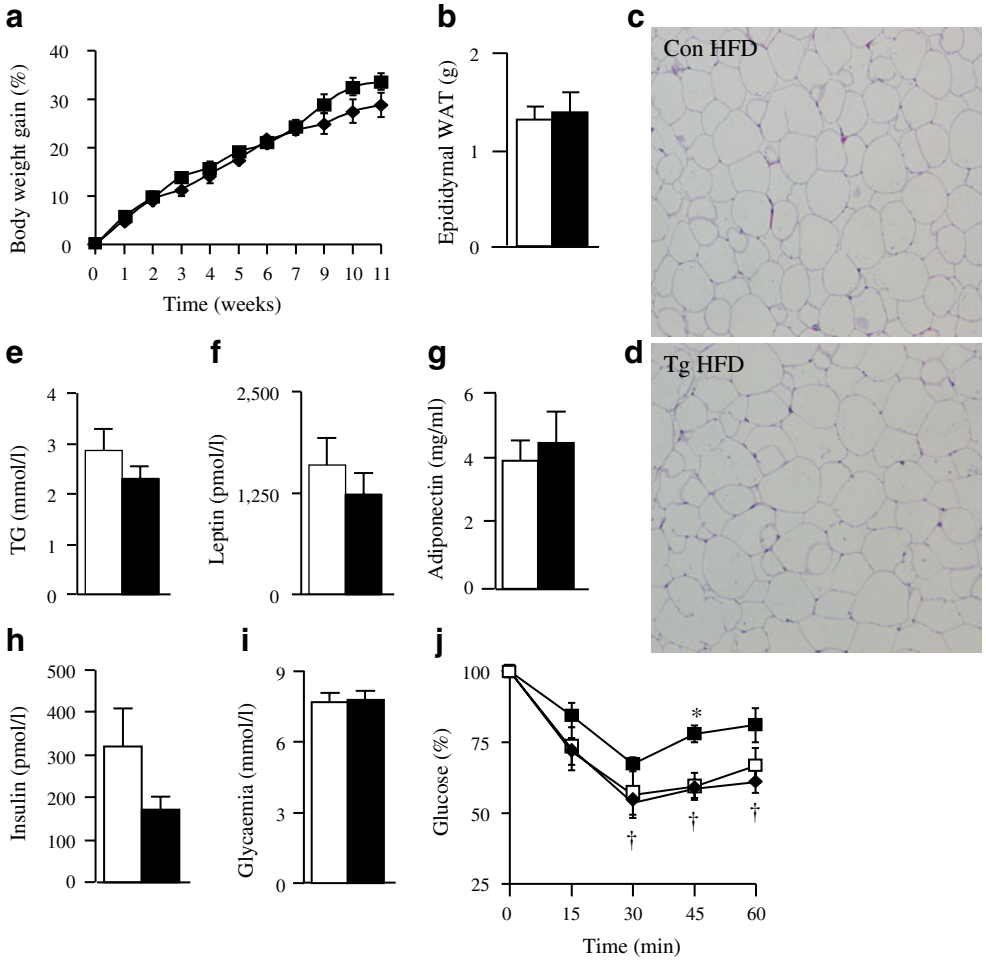

Fig. 9 Analysis of *Gck*-expressing transgenic mice fed a high-fat diet (HFD). Male control mice (Con) and transgenic (Tg) mice, 2 months old, were fed a high-fat diet for 11 weeks. **a** Body weight gain in fat-fed control mice (squares) and transgenic mice (diamonds). **b** Epididymal fat pad weight in fat-fed control (white bar) and transgenic (black bar) mice. **c, d** Representative haematoxylin/eosin sections of epididymal WAT from fat-fed control (**c**) and transgenic (**d**) mice (magnification ×10). **e–g** Circulating levels of serum triacylglycerol (TG) (**e**), leptin (**f**) and adiponectin (**g**) were measured in fat-fed control mice (white bars) and transgenic mice (black bars). **h, i** Circulating levels of serum insulin (**h**) and glucose (**i**) were measured in fat-fed control mice (white bars) and transgenic mice (black bars). **j** Results from the insulin tolerance test. Insulin, 0.375 U per kg body weight, was injected intraperitoneally into chow-fed control mice (white squares), fat-fed control mice (black squares) and fat-fed transgenic mice (black diamonds). Blood samples were taken from the tail veins of the same animals at the times indicated and glucose levels were determined. Results are means ± SEMs from at least seven mice for each group.*$p<0.05$ vs chow-fed controls; $^{\dagger}p<0.05$ vs high-fat-fed controls

Gck by glucose [38]. Therefore, our results are consistent with a view of adipose tissue as an active producer of lactate [39]. This is also in line with the results from microdialysis studies on humans showing a net release of lactate from adipose tissue after glucose ingestion [40–42]. The paradoxical increase of a gluconeogenic precursor in the postprandial state may be related to a possible role of lactate in insulin-dependent inhibition of lipolysis [43] as well as a liver glycogen or triacylglycerol precursor [44, 45]. In agreement with this, our results suggest that lactate released by adipose tissue is taken up by the liver, where it is converted to glycogen and triacylglycerol, without affecting circulating triacylglycerol and glucose levels.

Moreover, our results suggest that a chronic increase in circulating lactate levels does not lead to insulin resistance. It has been suggested that high levels of circulating lactate observed during obesity contribute to insulin resistance by decreasing glucose utilisation by skeletal muscle and enhancing hepatic gluconeogenesis [32–37]. Plasma lactate is elevated in obese individuals and this increase is higher when obesity is associated with type 2 diabetes [32]. A similar increase in plasma lactate is also observed in non-obese patients with type 2 diabetes [32, 36]. These increases are in the same range (about 50% increase) as those observed in our transgenic mice. Nevertheless, in the mice, whole-body and skeletal muscle insulin sensitivity and

glucose disposal were increased despite higher plasma lactate. Thus, our results indicate that high circulating lactate levels are probably not responsible for insulin resistance.

In our mice, improved glucose tolerance was probably due to increased glucose uptake by adipose tissue, and also to an increase in insulin-stimulated glucose uptake by skeletal muscle. This suggests that an increase in glucose uptake by adipose tissue, without any alteration in fat accumulation, probably led to the secretion of a factor able to regulate insulin sensitivity in skeletal muscle. However, in transgenic mice, no change was observed in circulating levels of hormones affecting glucose homeostasis such as adiponectin or leptin. Although other adipokines may be involved in the increased insulin sensitivity, the observed decrease in adipose tissue expression of *Rpb4* and serum levels of RPB-4, a crucial factor in the pathogenesis of insulin resistance, may have contributed to higher skeletal muscle insulin sensitivity. In agreement with this, *Glut4*-overexpressing transgenic mice also had decreased *Rbp4* expression [16]. However, although the regulation of RBP-4 production in WAT remains unclear, our results suggest that it is probably regulated not by lipid accumulation, but by glucose flux into adipose tissue.

Furthermore, despite increased glucose uptake in adipose tissue, transgenic mice expressing *Gck* did not accumulate more fat. *Gck* transgenic mice showed neither hypertrophy nor hyperplasia of adipose cells. In contrast, *Glut4*-overexpressing mice had adipocyte hyperplasia [18]. Nevertheless, despite the higher glucose incorporation into glycerol observed in transgenic mice overexpressing *Glut4*, their adipocytes did not show increased fat accumulation and 70% of glucose was metabolised to lactate [19]. Similarly, transgenic mice expressing *Gck* did not have increased fat accumulation and had higher lactate release by adipose tissue. Thus, the main difference between both transgenic models is the presence of adipose cell hyperplasia, which occurred only in *Glut4* transgenic mice, suggesting that an increase in glucose uptake by *Glut4* overexpression or by *Gck* expression may have different effects on immature adipocyte replication and/or differentiation.

The lack of excess fat accumulation in mice expressing *Gck* also highlights the potential dissociation between glucose uptake and triacylglycerol storage in adipose tissue. This agrees with the finding that in adipose-specific *Glut4* knockout mice, despite a marked decrease in adipose tissue glucose transport, no alteration in fat storage was observed [13]. This is also consistent with results obtained using labelled glucose, which indicate that uptake of glucose carbon in total body fat is in the order of less than 4% of glucose given [46]. This agrees with the finding that lactate and pyruvate may be utilised preferentially to glucose to produce glycerol for triacylglycerol deposition, and with a recent study in rats showing that quantitatively higher amounts of glycerol are gained, in response to sucrose feeding, from pyruvate/lactate via glyceroneogenesis than from glucose via glycolysis [7, 8, 47]. This suggests that glyceroneogenesis and glycolysis occur simultaneously in adipose tissue in the presence of increased glucose uptake by this tissue. Thus, a compartmentalisation of these pathways has been hypothesised, either in the same cell or in different adipose tissue cell types [7]. However, our data indicate that in adipose tissue expressing glucokinase, in which glucose uptake is increased, glyceroneogenesis decreased at high glucose concentration. Furthermore, this study suggests that in adipose tissue producing the enzyme HKII, glyceroneogenesis increased at high glucose due to the inhibition by glucose 6-phosphate. Therefore, glyceroneogenesis and glycolysis may occur in the same cell, but not at the same time, and the feedback inhibition of HKII by glucose 6-phosphate may permit glyceroneogenesis from lactate to occur after the activation of glycolysis.

In summary, our results suggest that an uncontrolled increase in glycolytic flux in adipose tissue leads to lactate production, rather than to higher glycerol 3-phosphate synthesis, fat accumulation and obesity. Furthermore, they suggest that a chronic increase in circulating lactate levels is not sufficient to lead to insulin resistance and point to the indirect pathway (glucose to lactate to glycerol 3-phosphate) as being key for fat deposition in adipose tissue.

Acknowledgements We thank: M. Watford for helpful discussions; C. H. Ros, M. Moya, M. Obach, D. Ramos, L. Noya and A. Vilalta for technical assistance; P. Iynedjian for the rat *Gck* cDNA and B. M. Spiegelman for the *aP2* promoter. S. Muñoz and A. Hidalgo received predoctoral fellowships from Direcció General d'Universitats, Generalitat de Catalunya, Spain. A. M. Monteys received a predoctoral fellowship from the Ministerio de Educación y Cultura, Spain. This study was supported by grants from Plan Nacional de I+D+I (SAF2002-20389 and SAF2005-01262) and Instituto de Salud Carlos III (CIBER de Diabetes y Enfermedades Metabólicas Asociadas), Spain and from the European Community (FP6 EUGENE2 [LSHM-CT-2004-512013]).

Duality of interest The authors declare that there is no duality of interest associated with this manuscript.

References

1. Ballard FJ, Hanson RW, Leveille GA (1967) Phosphoenolpyruvate carboxykinase and the synthesis of glyceride–glycerol from pyruvate in adipose tissue. J Biol Chem 242:2746–2750
2. Hanson RW, Reshef L (2003) Glyceroneogenesis revisited. Biochimie 85:1199–1205
3. Reshef L, Hanson RW, Ballard FJ (1969) Glyceride–glycerol synthesis from pyruvate. Adaptive changes in phosphoenolpyruvate carboxykinase and pyruvate carboxylase in adipose tissue and liver. J Biol Chem 244:1994–2001

4. Franckhauser S, Munoz S, Pujol A et al (2002) Increased fatty acid re-esterification by PEPCK overexpression in adipose tissue leads to obesity without insulin resistance. Diabetes 51: 624–630
5. Franckhauser S, Munoz S, Elias I, Ferre T, Bosch F (2006) Adipose overexpression of phosphoenolpyruvate carboxykinase leads to high susceptibility to diet-induced insulin resistance and obesity. Diabetes 55:273–280
6. Olswang Y, Cohen H, Papo O et al (2002) A mutation in the peroxisome proliferator-activated receptor gamma-binding site in the gene for the cytosolic form of phosphoenolpyruvate carboxykinase reduces adipose tissue size and fat content in mice. Proc Natl Acad Sci USA 99:625–630
7. Nye C, Kim J, Kalhan SC, Hanson RW (2008) Reassessing triglyceride synthesis in adipose tissue. Trends Endocrinol Metab 19:356–361
8. Nye CK, Hanson RW, Kalhan SC (2008) Glyceroneogenesis is the dominant pathway for triglyceride glycerol synthesis in vivo in the rat. J Biol Chem 283:27565–27574
9. Garvey WT, Maianu L, Huecksteadt TP, Birnbaum MJ, Molina JM, Ciaraldi TP (1991) Pretranslational suppression of a glucose transporter protein causes insulin resistance in adipocytes from patients with non-insulin-dependent diabetes mellitus and obesity. J Clin Invest 87:1072–1081
10. Herman MA, Kahn BB (2006) Glucose transport and sensing in the maintenance of glucose homeostasis and metabolic harmony. J Clin Invest 116:1767–1775
11. Koranyi L, James D, Mueckler M, Permutt MA (1990) Glucose transporter levels in spontaneously obese (db/db) insulin-resistant mice. J Clin Invest 85:962–967
12. Pedersen O, Kahn CR, Kahn BB (1992) Divergent regulation of the Glut1 and Glut4 glucose transporters in isolated adipocytes from Zucker rats. J Clin Invest 89:1964–1973
13. Abel ED, Peroni O, Kim JK et al (2001) Adipose-selective targeting of the GLUT4 gene impairs insulin action in muscle and liver. Nature 409:729–733
14. Kotani K, Peroni OD, Minokoshi Y, Boss O, Kahn BB (2004) GLUT4 glucose transporter deficiency increases hepatic lipid production and peripheral lipid utilization. J Clin Invest 114:1666–1675
15. Minokoshi Y, Kahn CR, Kahn BB (2003) Tissue-specific ablation of the GLUT4 glucose transporter or the insulin receptor challenges assumptions about insulin action and glucose homeostasis. J Biol Chem 278:33609–33612
16. Yang Q, Graham TE, Mody N et al (2005) Serum retinol binding protein 4 contributes to insulin resistance in obesity and type 2 diabetes. Nature 436:356–362
17. Gnudi L, Shepherd PR, Kahn BB (1996) Over-expression of GLUT4 selectively in adipose tissue in transgenic mice: implications for nutrient partitioning. Proc Nutr Soc 55:191–199
18. Shepherd PR, Gnudi L, Tozzo E, Yang H, Leach F, Kahn BB (1993) Adipose cell hyperplasia and enhanced glucose disposal in transgenic mice overexpressing GLUT4 selectively in adipose tissue. J Biol Chem 268:22243–22246
19. Tozzo E, Shepherd PR, Gnudi L, Kahn BB (1995) Transgenic GLUT-4 overexpression in fat enhances glucose metabolism: preferential effect on fatty acid synthesis. Am J Physiol 268: E956–E964
20. Katz A, Sahlin K, Broberg S (1991) Regulation of glucose utilization in human skeletal muscle during moderate dynamic exercise. Am J Physiol 260:E411–E415
21. Kubo K, Foley JE (1986) Rate-limiting steps for insulin-mediated glucose uptake into perfused rat hindlimb. Am J Physiol 250: E100–E102
22. Ren JM, Marshall BA, Gulve EA et al (1993) Evidence from transgenic mice that glucose transport is rate-limiting for glycogen deposition and glycolysis in skeletal muscle. J Biol Chem 268:16113–16115
23. Iynedjian PB (1993) Mammalian glucokinase and its gene. Biochem J 293:1–13
24. Ferre T, Riu E, Bosch F, Valera A (1996) Evidence from transgenic mice that glucokinase is rate limiting for glucose utilization in the liver. FASEB J 10:1213–1218
25. Ross SR, Graves RA, Greenstein A et al (1990) A fat-specific enhancer is the primary determinant of gene expression for adipocyte P2 in vivo. Proc Natl Acad Sci USA 87:9590–9594
26. Chevillotte E, Giralt M, Miroux B, Ricquier D, Villarroya F (2007) Uncoupling protein-2 controls adiponectin gene expression in adipose tissue through the modulation of reactive oxygen species production. Diabetes 56:1042–1050
27. Rodbell M (1964) Metabolism of isolated fat cells. I. Effects of hormones on glucose metabolism and lipolysis. J Biol Chem 239:375–380
28. Franckhauser S, Elias I, Rotter SV et al (2008) Overexpression of Il6 leads to hyperinsulinaemia, liver inflammation and reduced body weight in mice. Diabetologia 51:1306–1316
29. Otaegui PJ, Ferre T, Pujol A, Riu E, Jimenez R, Bosch F (2000) Expression of glucokinase in skeletal muscle: a new approach to counteract diabetic hyperglycemia. Hum Gene Ther 11:1543–1552
30. Salmon DM, Flatt JP (1985) Effect of dietary fat content on the incidence of obesity among ad libitum fed mice. Int J Obes 9:443–449
31. Koh YK, Lee MY, Kim JW et al (2008) Lipin1 is a key factor for the maturation and maintenance of adipocytes in the regulatory network with CCAAT/enhancer-binding protein alpha and peroxisome proliferator-activated receptor gamma 2. J Biol Chem 283:34896–34906
32. Chen YD, Varasteh BB, Reaven GM (1993) Plasma lactate concentration in obesity and type 2 diabetes. Diabète Métab 19:348–354
33. Choi CS, Kim YB, Lee FN, Zabolotny JM, Kahn BB, Youn JH (2002) Lactate induces insulin resistance in skeletal muscle by suppressing glycolysis and impairing insulin signaling. Am J Physiol Endocrinol Metab 283:E233–E240
34. Lombardi AM, Fabris R, Bassetto F et al (1999) Hyperlactatemia reduces muscle glucose uptake and GLUT-4 mRNA while increasing (E1alpha)PDH gene expression in rat. Am J Physiol 276:E922–E929
35. Lovejoy J, Newby FD, Gebhart SS, DiGirolamo M (1992) Insulin resistance in obesity is associated with elevated basal lactate levels and diminished lactate appearance following intravenous glucose and insulin. Metabolism 41:22–27
36. Reaven GM, Hollenbeck C, Jeng CY, Wu MS, Chen YD (1988) Measurement of plasma glucose, free fatty acid, lactate, and insulin for 24 h in patients with NIDDM. Diabetes 37:1020–1024
37. Vettor R, Lombardi AM, Fabris R et al (1997) Lactate infusion in anesthetized rats produces insulin resistance in heart and skeletal muscles. Metabolism 46:684–690
38. Printz RL, Magnuson MA, Granner DK (1993) Mammalian glucokinase. Annu Rev Nutr 13:463–496
39. DiGirolamo M, Newby FD, Lovejoy J (1992) Lactate production in adipose tissue: a regulated function with extra-adipose implications. FASEB J 6:2405–2412
40. Frayn KN, Coppack SW (1990) Evidence for lactate production by human adipose tissue in vivo. Diabetologia 33:740–741
41. Hagstrom E, Arner P, Ungerstedt U, Bolinder J (1990) Subcutaneous adipose tissue: a source of lactate production after glucose ingestion in humans. Am J Physiol 258:E888–E893

42. Jansson PA, Smith U, Lonnroth P (1990) Evidence for lactate production by human adipose tissue in vivo. Diabetologia 33:253–256
43. Ahmed K, Tunaru S, Tang C et al (2010) An autocrine lactate loop mediates insulin-dependent inhibition of lipolysis through GPR81. Cell Metab 11:311–319
44. Newgard CB, Hirsch LJ, Foster DW, McGarry JD (1983) Studies on the mechanism by which exogenous glucose is converted into liver glycogen in the rat. A direct or an indirect pathway? J Biol Chem 258:8046–8052
45. Newgard CB, Moore SV, Foster DW, McGarry JD (1984) Efficient hepatic glycogen synthesis in refeeding rats requires continued carbon flow through the gluconeogenic pathway. J Biol Chem 259:6958–6963
46. Marin P, Rebuffe-Scrive M, Smith U, Bjorntorp P (1987) Glucose uptake in human adipose tissue. Metabolism 36:1154–1160
47. Francendese AA, DiGirolamo M (1981) Alternative substrates for triacylglycerol synthesis in isolated adipocytes of different size from the rat. Biochem J 194:377–384